Formation of $C_7H_7^+$ from Benzyl Chloride and Chlorotoluene Molecular Ions: A Theoretical Study

Joong Chul Choe*

Department of Chemistry, Dongguk University, Seoul 100-715, Korea

Received: March 27, 2008; Revised Manuscript Received: April 24, 2008

The potential energy surface (PES) for the formation of $C_7H_7^+$ from benzyl chloride and chlorotoluene ions was obtained by quantum chemical calculations at the B3LYP/6-311+G(3df,2p)//B3LYP/6-31G(d) level. On the basis of the PES, the RRKM model calculations were carried out to predict the rate constants of the dissociations of the molecular ions of *o*-, *m*-, and *p*-chlorotoluene, all of which agreed well with previous experimental results. The kinetic analysis showed that the benzylium ion was the predominant product in the dissociations of the four isomeric molecular ions, below the thresholds of the formation of tolylium ions.

1. Introduction

The toluene molecular ion and its derivatives can produce the benzylium ion (**Bz**) and tropylium ion (**Tr**) by gas-phase unimolecular dissociation. Their kinetics and mechanisms have been studied extensively for half a century since the pioneering work by Rylander et al.[1] The dissociation of halogen-substituted toluene ions has been investigated using various experimental methods.[2–16] The main interest of the studies is the structural identification of the $C_7H_7^+$ product ions formed by loss of a halogen atom. In the dissociation of halotoluene ions, one should consider the tolylium ion additionally as a $C_7H_7^+$ product ion. The dissociation rate constants of chloro-, bromo-, and iodotoluene ions were measured with a photoelectron−photoion coincidence (PEPICO) method.[2] Those of bromo- and/or iodotoluene ions were measured using a time-resolved photodissociation (TRPD) method, based on Fourier transform ion cyclotron resonance (FT-ICR) spectrometry,[3–6] and photodissociation using mass-analyzed ion kinetic energy spectrometry (PD-MIKES).[7,8] In the PD-ICR study for isomeric bromotoluene ions, Shin and co-workers demonstrated that **Bz** is produced exclusively below the threshold of the formation of tolylium ion.[4] They proposed that the dissociation pathway to **Bz** via the brominated isotoluene (methylene cycloheptadiene) ions would be favored kinetically over the pathway to **Tr**, via a ring expansion.

In this work, we investigate the dissociation mechanism of isomeric chlorinated toluene ion derivates, a mechanism that would be similar to that of the toluene ion. It is well-known that the toluene ion produces **Bz** and **Tr** by a direct C−H bond cleavage and via a ring expansion, respectively.[17–19] To produce **Tr**, the toluene ion goes through three intermediates: the distonic benzenium ion (**b**); the norcaradiene ion (**c**); and the cycloheptatriene ion (**d**) (Scheme 1). Lifshitz and co-workers carried out a kinetic analysis by a Rice−Rampsperger−Kassel−Marcus.

(RRKM) modeling[20] based on the quantum chemically calculated potential energy surface (PES) and explained successfully the experimental data including dissociation rate constants and **Bz**/**Tr** abundance ratios.[18] The analogous mechanisms have been used for understanding the formation of $C_7H_7^+$ from various toluene ion derivatives, including alkylbenzene and halotoluene ions.[21–25]

Recently, we proposed another dissociation channel to produce **Bz** from the toluene ion (Scheme 1).[26] The density functional molecular orbital (MO) calculations showed that the energy barrier for the isomerization, **b** → *o*-isotoluene ion (**e**), is comparable with that for **b** → **c**. The RRKM model calculations predicted that **Bz** formation via the isomeric isotoluene ions is not less significant than that occurring by the direct C−H bond cleavage. Recently, an analogous mechanism was adopted to understand the formation of $C_7H_7^+$ from the methyl-substituted toluene ions, ethylbenzene, and xylene ions.[27] According to the results, the ethylbenzene ion can produce **Bz** and **Tr** by a direct C−C bond cleavage and via a ring expansion, respectively. The methylated isotoluene ions are not important intermediates in the dissociation. On the other hand, without involvement of the methylated isotoluene ions, the **Bz** formation from *o*-, *m*-, and *p*-xylene ions, suggested by the MIKES experiments,[25] could not be explained. It is highly probable that the dissociation mechanisms of the benzyl chloride ion (**1a**) and chlorotoluene ions parallel those of ethylbenzene and xylene ions. In this work, the PES for the dissociation of **1a**, *o*-, *m*-, and *p*-chlorotoluene ions (**2a**, **3a**, and **4a**, respectively) was obtained by density functional theory (DFT) calculations. The dissociation rate constants of **2a**−**4a** were predicted by RRKM model calculations, which will be compared to the previous experimental data. From the calculated PES and rate constant results the dissociation mechanism will be discussed.

2. Computational Methods

The MO calculations were performed with the Gaussian 03 suite of programs.[28] Geometry optimizations for the stationary points were carried out at the unrestricted B3LYP level of density functional theory (DFT) using the 6-31G(d) basis set. TS geometries connecting the stationary points were searched and checked by calculating the intrinsic reaction coordinates at the same level. For increased accuracy of the energies, single-point energy calculations were carried out at the B3LYP/6-311+G(3df,2p) level. The harmonic frequencies calculated at the B3LYP/6-31G(d) level and scaled down by 0.9806[29] were used for zero-point vibrational energy (ZPVE) corrections.

* Corresponding author. E-mail: jcchoe@dongguk.edu.

10.1021/jp802641c CCC: $40.75
Published on Web 06/11/2008

SCHEME 1

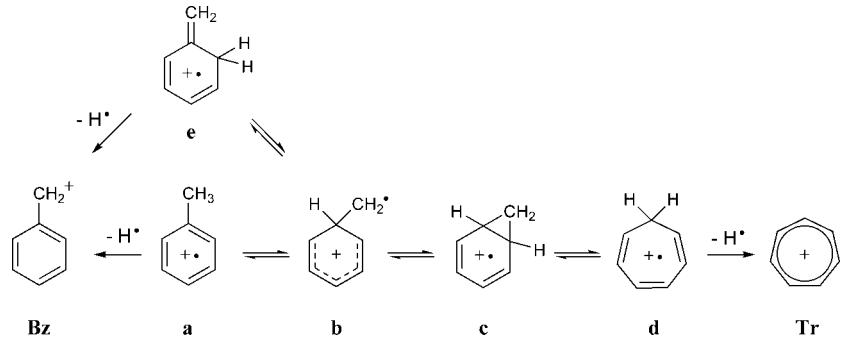

The RRKM expression was used to calculate the rate-energy dependences[20]

$$k(E) = \frac{\sigma N^{\neq}(E - E_0)}{h\rho(E)} \quad (1)$$

where E is the reactant internal energy, E_0 the critical energy of the reaction, $N^{\neq}$ the sum of the TS states, ρ the density of the reactant states, and σ the reaction path degeneracy. $N^{\neq}$ and ρ were evaluated by a direct count of states using the Beyer−Swinehart algorithm.[30]

3. Results and Discussion

By a direct C−Cl bond cleavage, **1a** can produce **Bz**, whereas **2a**−**4a** can produce the *o*-, *m*-, and *p*-tolylium ions, respectively. We could not locate the TSs for these bond cleavage reactions, indicating that the dissociations occur via loose TSs without reverse barriers. The endoergicities obtained by the B3LYP/6-311+G(3df,2p)//B3LYP/6-31G(d) calculations for the formation of *o*-, *m*-, and *p*-tolylium ion from **2a**−**4a** by loss of Cl• are 318, 326, and 348 kJ mol^{-1}, respectively. Since these are much higher than the critical energies (around 170 kJmol^{-1}) for the formation of **Bz** and **Tr**, we will not consider the formation of the isomeric tolylium ions here. Note that, however, the tolylium ions can be produced from the chlorotoluene ions at much higher energy than their thresholds, due in general to the fact that a direct bond cleavage becomes more favored kinetically than a rearrangement reaction with increasing energy.

Benzyl Chloride Ion. As expected, the dissociation pathway of **1a** was parallel to those of the toluene[31] and ethylbenzene[27] ions reported recently. A hydrogen atom of the CH_2Cl group can migrate to the ipso position to form an important intermediate having the distonic benzenium structure, **1b** (Scheme 2a). Species abbreviation follows the notation of the previous work on ethylbenzene and xylene ions.[27] Either the CHCl group or the ipso H atom of **1b** can move toward one of the adjacent carbons. The movement of the former forms the chlorinated norcaradiene ion, **1c**, and that of the latter forms the chlorinated isotoluene ions, **1e** and **1i**. These pathways are shown in parts a and b of Scheme 2, respectively. The schemes include the relative energies of the stable species and the TSs connecting them with respect to **2a**, calculated at the B3LYP/6-311+G-(3df,2p)//B3LYP/6-31G(d) level. **1c** can produce **Tr** by loss of Cl• via the cycloheptatrienyl chloride ion, **1d**. **1e** or **1i** can form other chlorinated isotoluene isomers such as **1f**, **1g**, and **1h** by an "H ring walk". The isomerizations to the chlorinated isotoluene ions do not contribute to the **Bz** or **Tr** formation directly.

The energy barriers for such rearrangements are higher than that for the direct C−Cl bond cleavage for the **Bz** formation (see the potential energy diagram in Figure 1). These energetics

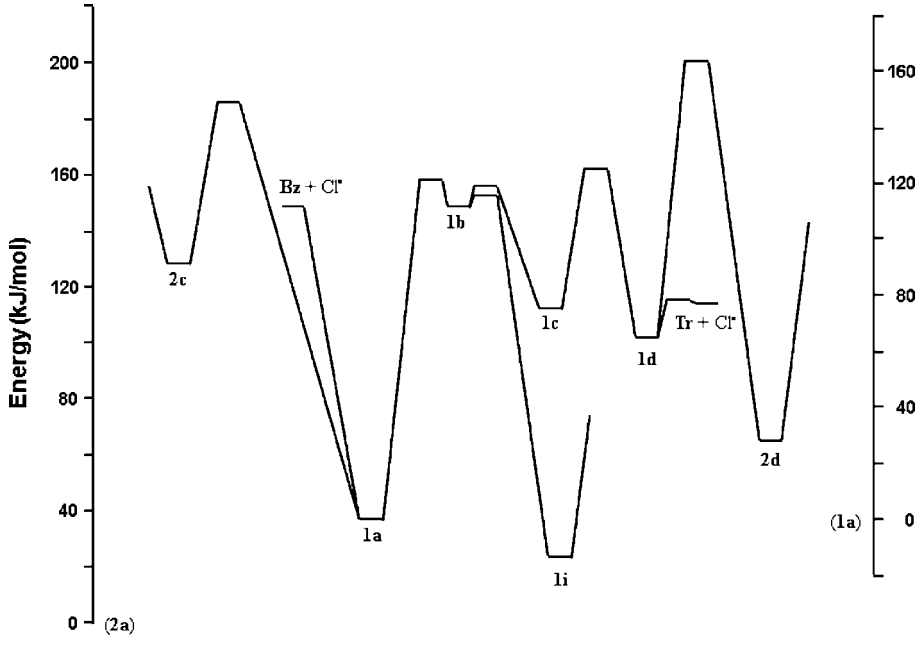

Figure 1. Potential energy diagram for isomerization and dissociation of the benzyl chloride ion derived from the B3LYP/6-311+G(3df,2p)// B3LYP/6-31G(d) calculations. The pathway to form the chlorinated isotoluene ions is approximated by one-well potential for convenience.

SCHEME 2: Isomerization and Dissociation Pathways of (a) 1a−4a and (b) 1b−4b Obtained by B3LYP/6-31G(d) Calculations[a]

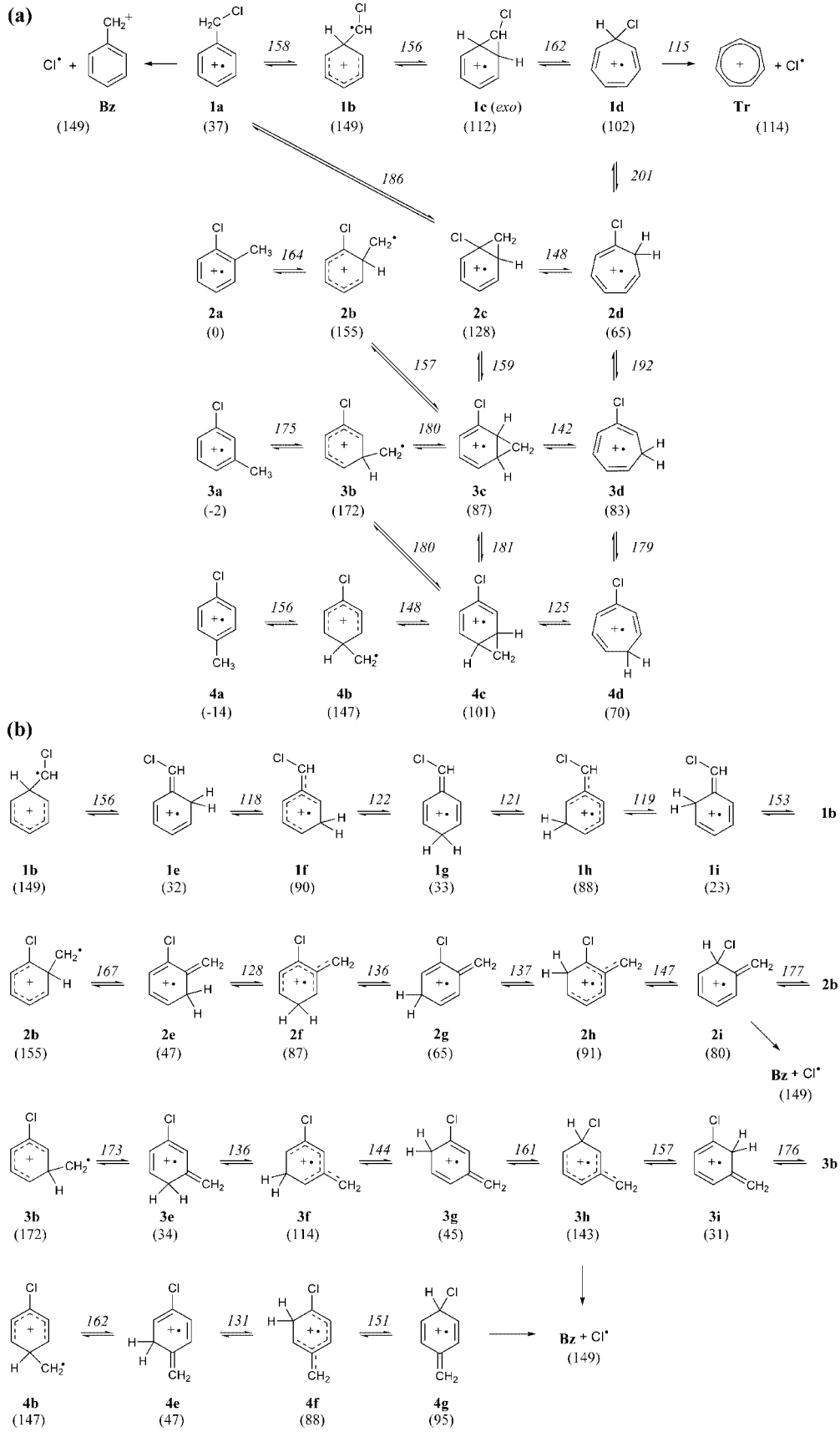

[a] The relative energies calculated at the B3LYP/6-311+G(3df,2p)//B3LYP/6-31G(d) level are denoted in the parentheses and above the arrows for the stable species and TSs, respectively. The calculated and scaled ZPVE corrections are included.

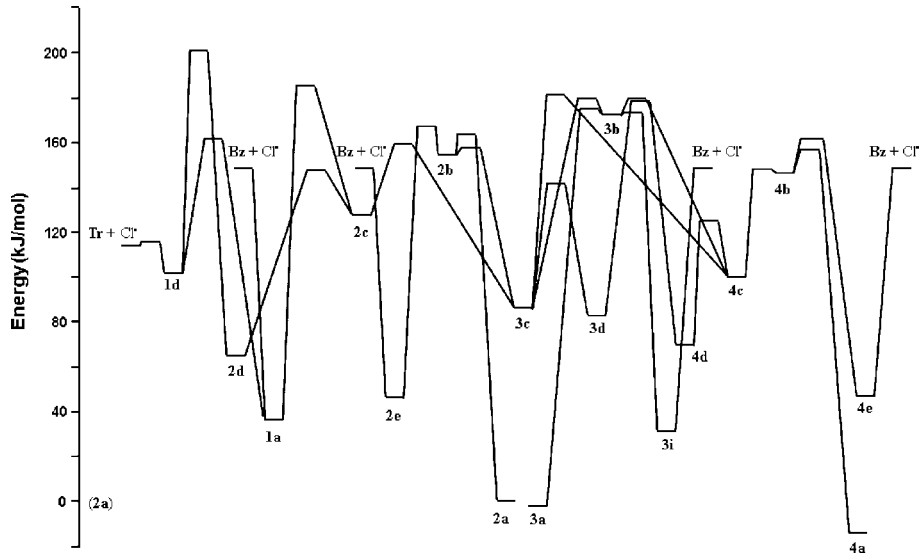

Figure 2. Same as Figure 1 for the *o*-, *m*-, and *p*-chlorotoluene ions. The pathways from **2b**, **3b**, and **4b** to **Bz** + Cl• via the chlorinated isotoluene ions are approximated by one-well potentials for convenience. The direct pathway from **2d** to **3d** via **TS2d3d** (192 kJ mol^{-1}) is not included.

SCHEME 3

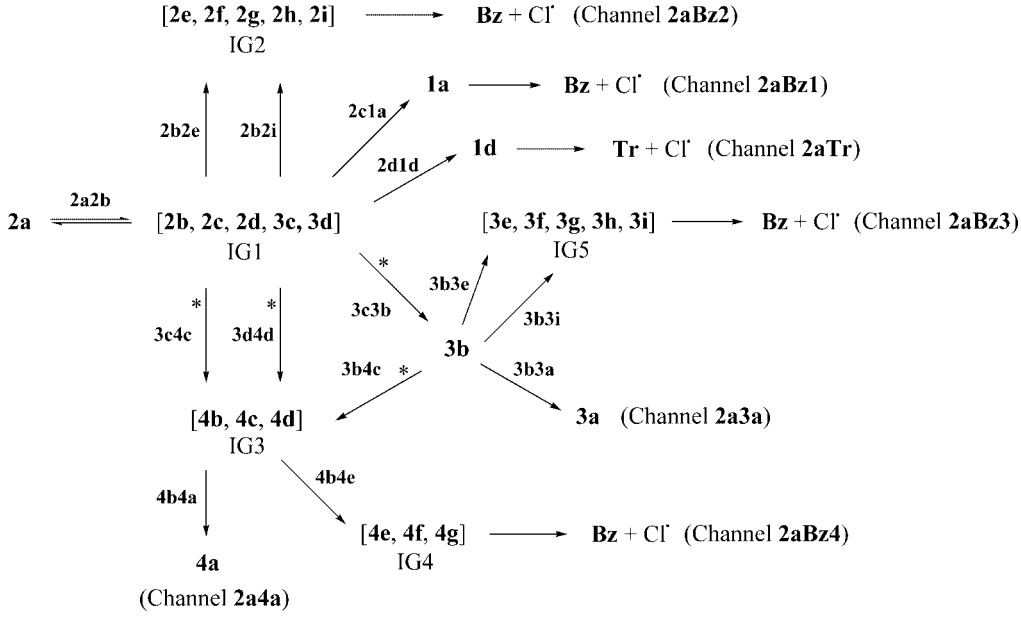

are different from those for the dissociations of toluene and ethylbenzene ions in which the critical energies for **Bz** formation are higher than for the formation of **Tr** or isotoluene ions, implying that the formation of **Bz** is much more favorable than that of **Tr** in the dissociation of **1a**. According to rough RRKM rate calculations, the former occurs faster than the latter by more than 10^5 from the threshold up to 500 kJ mol^{-1} of the internal energy, indicating that **1a** produces **Bz** exclusively through loss of Cl•, whereas both of **Bz** and **Tr** are formed competitively in the dissociations of toluene and ethylbenzene ions. The other pathways to form **2c** or **2d**, starting from **1a**, which will be described below, are also much less favorable than the **Bz** formation (Figure 1).

In a photoionization (PI) study, Traeger and Kompe proposed that **Tr** is formed from benzyl halide (Cl, Br, I) ions at the threshold and that the **Bz** formation occurs dominantly when it becomes energetically possible.[14] With only the electronic ground surface obtained here, the proposed **Tr** formation can not be explained. One might think that it occurs through quantum mechanical tunneling below the rearrangement barriers in the present PES. However, the dissociation by tunneling is usually observed only when movement of a light particle, such as H, is involved, which is not in this case here.[20,31–33] From collision-induced dissociation (CID)[9–12] and ICR[13] studies, it was reported that 80−93% of the $C_7H_7^+$ ions formed from **1a** have the benzylium structure. It is highly probable that the minor product is **Tr** formed by the further isomerization of **Bz** after formation at high energy. Similarly, Fridgen et al. reported that **Bz** formed from the ethylbenzene ion can undergo isomerization to **Tr**.[34] According to their calculation, **Bz** can isomerize to **Tr** via the intermediate, the norcaradienyl ion, which is a mechanism simpler than that suggested by Cone et al.[35]

Chlorotoluene Ions. ***PES.*** A hydrogen atom of the CH_3 group of the optimized **2a** or **3a** is in the plane of the benzene ring, whereas that of **4a** lies vertical to the benzene ring. The chlorinated distonic benzenium ions, **2b**−**4b**, formed from the three chlorotoluene ions, can undergo two types of rearrangements. Movement of the CH_2 groups leads to the ring expansions via the chlorinated norcaradiene ions, **2c**−**4c** (Scheme 2a). The TS connecting **2b** and **2c**, unfortunately, could not be located.

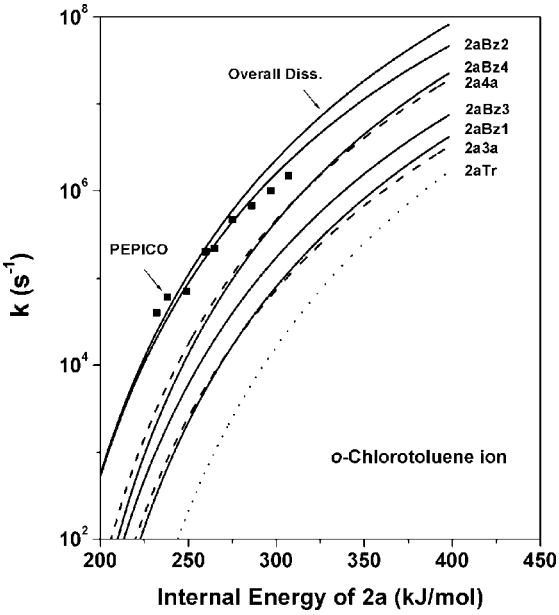

Figure 3. Rate-energy dependences for the individual reaction channels (see Scheme 3) and overall dissociation of *o*-chlorotoluene ion. Curves are the result of RRKM model calculations. Rectangular points are the PEPICO result.[2]

2b isomerizes to **2c** via the more stable intermediate, **3c**, and by migration of the CH_2 group, **2c**−**4c** can be interconvertible. Each of the 1,2-CH_2 shifts occurs through the TS (**TS2c3c** or **TS3c4c**) of which the CH_2 group lies vertical to the benzene ring. When the CH_2 group of 3c moves toward other directions, **2b** or **3b** is formed, of which the CH_2 group is nearly in the plane of the benzene ring. In this way, the isomerization of **3c** and **4c** can occur by a concerted or a two-step mechanism with similar barrier heights. **2c** can isomerize to **1a** by a rearrangement, which was not found in the previous study on the dissociation of ethylbenzene and xylene ions.[27] As a C−C bond of the CH_2 group of 2c is broken, the Cl atom and the CH_2 group move away from and toward the plane of the benzene ring, respectively, and **TS2c1a** is formed. After passing the TS, the C−Cl bond distance increases and eventually the Cl atom shifts to the CH_2 group to form **1a**. **1a** undergoes the dissociation to Bz + $Cl^•$ exclusively as described above. By the ring expansion, each of **2c**−**4c** can form the seven-membered ring isomers, **2d**−**4d**, respectively. **1d**−**4d** can isomerize also to each other by an H ring walk. Through the isomerization **2d** → **1d**, Tr can be produced. Alternatively, each of **2b**−**4b** can undergo an H ring walk to various isomers having the isotoluene structure and eventually dissociate to Bz + $Cl^•$ (Scheme 2b). Namely, there are two types of pathway to produce Bz from **2a**−**4a**, via **1a** or by way of the isotoluene ion derivatives. If only the energetics is considered, the pathways of the latter type will be more favorable (Figure 2). There are also two types of pathways to produce Tr from the chlorotoluene ions. One is via **2c** and **1a** and the other through **2d** and **1d**. The energy diagram in Figure 2, however, shows that both the pathways are less favorable than those to produce Bz, which will be confirmed by a kinetic analysis below.

RRKM Model Calculations. As described above, the chlorotoluene ions should undergo several isomerization steps prior to dissociation. The pathways other than the minimum energy reaction pathway (MERP) can contribute to the formation of $C_7H_7^+$, since the dissociation kinetics is determined by the entropic factor as well as by the energetic factor. We carried out RRKM rate calculations for the formation of $C_7H_7^+$ from each of **2a**−**4a** to find out the major product and to estimate the contributions of each dissociation pathway. As seen in Figure 2, the PES is too complicated for thorough analysis of the dissociation kinetics without proper approximations. Under a few assumptions, the individual contributions to the product $C_7H_7^+$ ions of the several dissociation channels as well as the overall dissociation rate constants that will be compared to the previous PEPICO data[2] can be obtained.

The starting molecular ions, **2a**−**4a** are much more stable than most of the other intermediates, meaning that the reactions occurring from the intermediates are much faster than the first step of the dissociation, for example, **2a** → **2b** in the dissociation of **2a**. For this reason the steady-state approximation can be used. Consider a reaction that produces several products, P_is from reactant A, via a common intermediate, I, having very short lifetime With the steady-state approximation, the rate

$$\mathrm{A} \xrightarrow{k_a} \mathrm{I} \begin{cases} \xrightarrow{k_1} \mathrm{P_1} \\ \xrightarrow{k_2} \mathrm{P_2} \\ \xrightarrow{k_i} \mathrm{P_i} \end{cases} \qquad (2)$$

constant to produce P_i is determined by

$$k_{p,i} = k_a f_i \qquad (3)$$

where f_i is the fraction of the i channel given by

$$f_i = \frac{k_i}{\sum_i k_i} \qquad (4)$$

The overall rate constant is the sum of $k_{p,i}$s and the abundance of P_i is proportional to $k_{p,i}$.When the backward isomerization I → A is competitive to other forward reactions, its rate constant should be added to the sum in the denominator of eq 4. The reaction can be more complicated. When there is another pathway to form I from A, for example A → B → I, its rate constant should be added to k_a of eq 3. When an unstable P_i undergoes further parallel reactions to Q_js, the rate constant to produce Q_j is given by $k_a f_i f_j$ where f_j is the fraction of the j channel out of reactions from P_i.

Scheme 3 shows the approximated dissociation pathway of **2a** used in the RRKM calculation. Some intermediates can interconvert rapidly prior to their further reactions, which will be called an intermediate group (IG) here and treated as a common intermediate. There are five IGs in the dissociation pathways of **2a**, as shown in Scheme 3. IG1, IG3, and **3b** are branching intermediates that undergo several parallel reactions. Since the rate constants of the further reactions are far larger than that of the first step, **1a** → **1b**, the steady-state approximation described above can be employed. All the reactions are categorized as five dissociations (to **Bz** and **Tr**) and two isomerizations (to **3a** and **4a**) channels. These seven channels can be treated as parallel reactions with their product abundances determined by their individual rate constants.

First, we calculated the RRKM rate constants (eq 1) for the individual steps with the TSs as denoted next to the arrows in Scheme 3. For example, **2a2b** means the TS connecting **2a** and **2b**. The steps for which no TSs are indicated are the reactions occurring very fast, which do not affect the rate constants of the individual channels. The critical energies and vibrational frequencies obtained from the present DFT calculation were used in the RRKM calculation. The vibrational frequencies of all the reactants and TSs were scaled down by 0.9614.[29] From these calculated

SCHEME 4

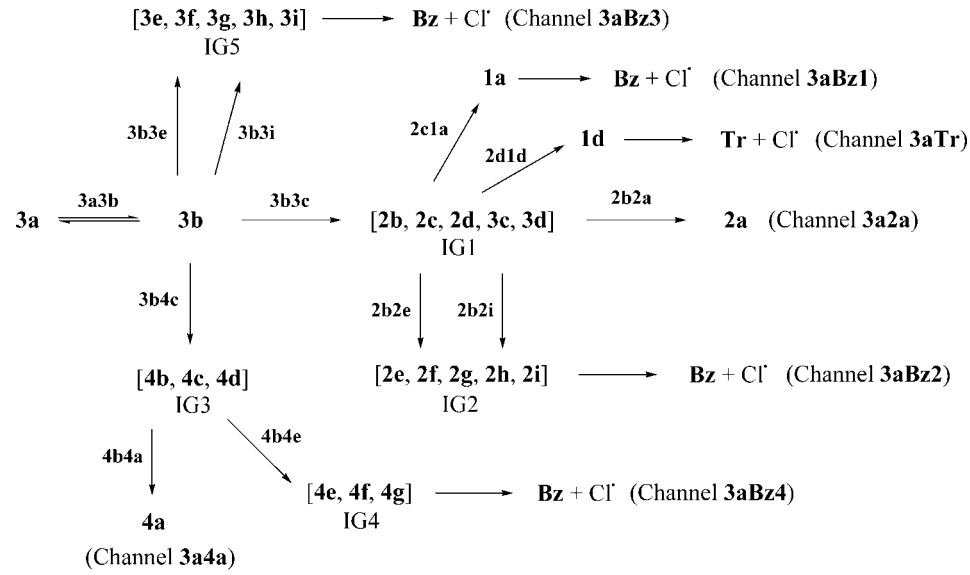

individual rate constants, we obtained the rate constants of the seven channels using the above steady-state method. The obtained rate-energy dependences are shown in Figure 3. The fastest channel was channel **2aBz2**, occurring via the isotoluene ions chlorinated at the ortho position, which is the MERP required to produce **Bz** starting from **2a**, indicating that Channel **2aBz2** is the main dissociation pathway. The secondary important dissociation pathway is channel **2aBz4**, occurring via the isotoluene ions chlorinated at the para position. The other two channels that produce **Bz** (channels **2aBz3** and **2aBz1**) contribute to the dissociation less than 10%. The contribution of channel **2aTr** producing **Tr** is negligible. Even though **1a** formed from IG1 can produce **Tr**, it produces **Bz** exclusively as mentioned above. The rate-energy dependence for the overall dissociation, the sum of the five dissociation channels, is shown in Figure 3. It agrees well with the previous PEPICO results[2] considering the approximations used here. The result shows that some of **1a** ions isomerize to **4a** by channel **2a4a** and the isomerization to **3a** by channel **2a3a** hardly occurs.

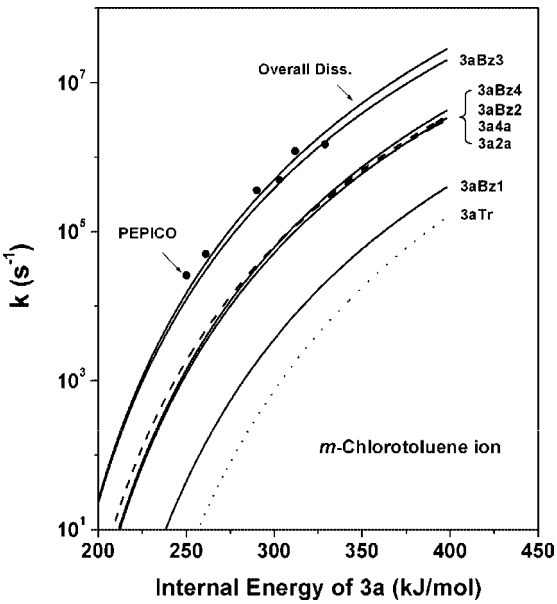

Figure 4. Rate-energy dependences for the individual reaction channels (see Scheme 3) and overall dissociation of *m*-chlorotoluene ion. Curves are the result of RRKM model calculations. Circular points are the PEPICO result.[2]

Some backward isomerization steps other than the first, IG1 → **2a**, are competitive toward further reactions. Their corresponding forward steps are denoted by asterisks in Scheme 3. If such backward steps are considered, the rate constants for channels **2aBz1**, **2aBz2**, and **2aTr** will become somewhat larger than those depicted in Figure 3, whereas those for the other channels will become smaller. The differences were estimated to be approximately 10% relatively. The difference in the overall dissociation constant, however, is much smaller since it originates only from channels **2a3a** and **2a4a**. For the same reason, the backward isomerization steps other than the first ones were not considered in the RRKM calculations for the reactions starting from **3a** and **4a** described below. Even though the present calculation is not as exact as those by solving the exact kinetic equations, it is useful to understand the reaction mechanism and useful enough to compare the theoretical results with the experimental data.

For the reactions starting from **3a** and **4a**, the rate constants were calculated the same way. The approximated pathways of the reactions are shown in Schemes 4 and 5, respectively. The RRKM rate-energy dependences for the individual reaction channels and the overall dissociation of **3a** are shown in Figure 4. The main dissociation channel is **3aBz3**, occurring via the isotoluene ions chlorinated at the meta position, which is the MERP to produce **Bz** starting from **3a**. The rate constants of the minor reactions occurring by channels **3aBz2**, **3aBz4**, **3a2a**, and **3a4a** are similar. The former two are the dissociations to **Bz**, and the latter two are the isomerizations to **2a** and **4a**. The contributions of the dissociations to **Bz** via **1a** and to **Tr** are negligible. The calculated overall dissociation rate constants agree well with the PEPICO data.[2] Figure 5 shows the rate-energy dependences for the reactions starting from **4a**. The dominant dissociation pathway is channel **4aBz4**, occurring via the isotoluene ions chlorinated at the para position, which is the MERP that produces **Bz** starting from **4a**. The other dissociation and isomerization channels are far less important. The calculated overall dissociation rate constants agree well with the PEPICO data.[2]

The rate-energy dependences for the dissociations of **2a**−**4a** are shown together in Figure 6. The dissociation rate of **2a** is

SCHEME 5

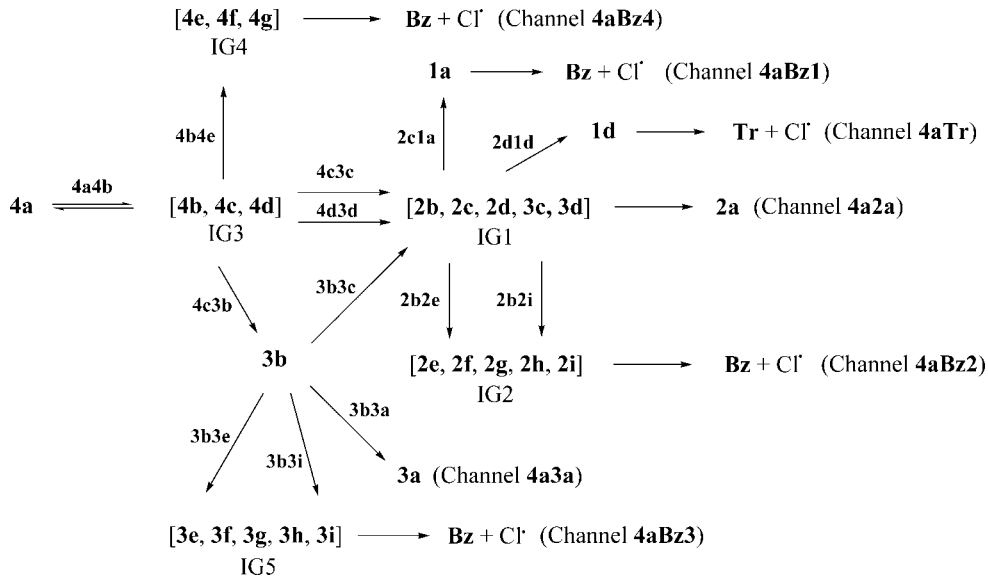

faster than those of **3a** and **4a**. As described above, the mechanisms of the main dissociation channels are similar for **2a**−**4a**, which are the formation of **Bz** via the chlorinated isotoluene ions. The difference in dissociation rates is mainly due to the reaction barrier. The barriers of the MERPs to produce **Bz** from **2a**−**4a** are 167, 177, and 176 kJ mol^{-1}, respectively. The lower barrier of **2a** makes the dissociation faster. Olesik et al.[2] fit their PEPICO data by an RRKM model calculation assuming that the dissociation occurs by one step. From the best fit, they obtained the critical energies for the dissociations of **2a**−**4a** as 164, 171, and 171 kJ mol^{-1}, respectively, which were somewhat lower than the respective barriers of the MERPs to produce **Bz**. The slopes of the present RRKM rate curves vs energy are somewhat steeper than those of experimental data, showing that the TSs are actually tighter than those used in the present calculation. Therefore, to achieve the better fitting, one should use lowered critical energies and tighter TSs. In the present RRKM calculation, the calculated vibrational frequencies of TSs were scaled by 0.9614. This scaling factor has been recommended for stable species, not TSs. When one scales these by the value larger than 0.9614, the TSs become tighter and one would obtain the better rate curve fitting. The use of the larger scaling factor for TSs has been often reported,[26,34,36] and since there can be several adjustable cases for the best fit, the better fitting is mentioned only qualitatively.

From the ICR study, Jackson et al.[13] reported that 96% of the $C_7H_7^+$ ions produced by ionization of *p*-chlorotoluene have the **Bz** structure, which agrees well with the present result. The benzylium ions produced can further isomerize to **Tr** when they have high internal energy, which is the main reason for the low

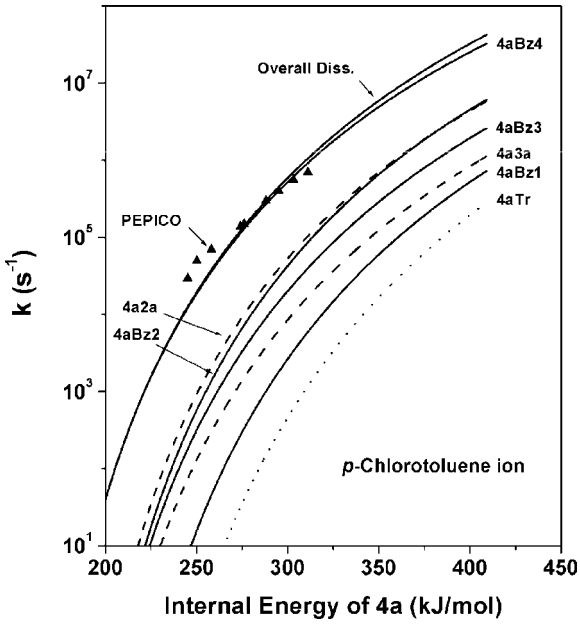

Figure 5. Rate-energy dependences for the individual reaction channels (see Scheme 3) and overall dissociation of *p*-chlorotoluene ion. Curves are the result of RRKM model calculations. Triangular points are the PEPICO result.[2]

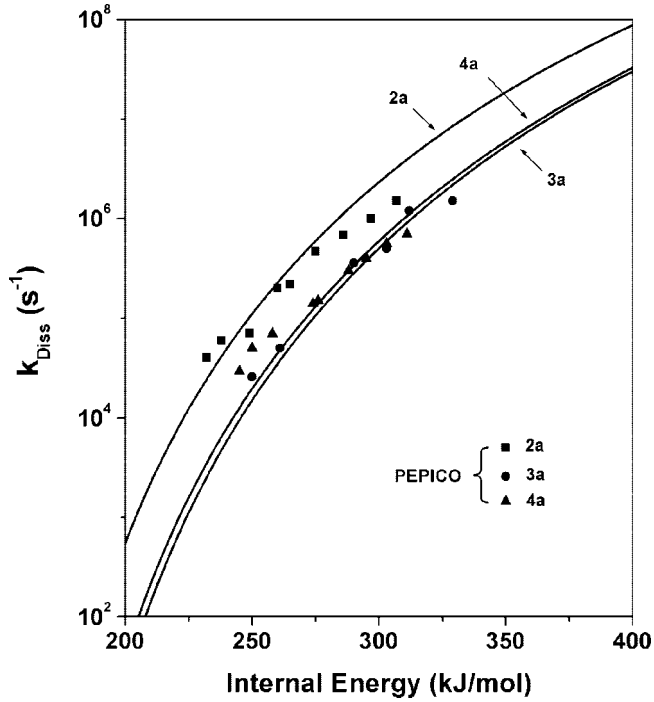

Figure 6. Rate-energy dependences for the dissociation of *o*-, *m*-, and *p*-chlorotoluene ions (**2a**, **3a**, and **4a**, respectively). Curves are the result of RRKM model calculations. Points are the PEPICO result.[2]

relative abundances of **Bz** determined by CID experiments for the chlorotoluene ions generated by 70-eV ionization.[9–12]

4. Conclusion

The PES for dissociation and isomerization of **1a**−**4a** was obtained by the B3LYP/6-311+G(3df,2p)//B3LYP/6-31G(d) calculations. The RRKM model calculations were carried out to obtain the dissociation rate constants. For all the molecular ions, the only dissociation $C_7H_7^+$ product was **Bz**. From **1a**, **Bz** was produced by the direct C−Cl bond cleavage. In the reactions of **2a**−**4a**, the rearrangements to the chlorinated isotoluene ions followed by the C−Cl bond cleavage were the main dissociation mechanisms to produce **Bz**. Their dissociation rates were much faster than their interconversion. The calculated rate constants of the dissociation of **2a**−**4a** agreed well with the previous PEPICO experimental data.

Acknowledgment. This work was supported by the Korea Research Foundation Grant funded by the Korean Government (MOEHRD) (KRF-2007-313-C00351). The author would like to acknowledge the support from KISTI Supercomputing Center (KSC-2007-S00-1026). The author also thanks Min Kyoung Yim for assistance in theoretical calculations. Dedicated to Professor Myung Soo Kim on the occasion of his 60th birthday.

References and Notes

(1) Rylander, P. N.; Meyerson, S.; Grubb, H. M. *J. Chem. Phys.* **1957**, *79*, 842.
(2) Olesik, S.; Baer, T.; Morrow, J. C.; Ridal, J. J.; Buschek, J.; Holmes, J. L. *Org. Mass Spectrom.* **1989**, *24*, 1008.
(3) Shin, S. K.; Han, S. J.; Kim, B. *Int. J. Mass Spectrom. Ion Processes* **1996**, *157*, 345.
(4) Kim, B.; Shin, S. K. *J. Chem. Phys.* **1997**, *106*, 1411.
(5) Kim, B.; Shin, S. K. *J. Phys. Chem. A* **2002**, *106*, 9918.
(6) Shin, S. K.; Kim, B.; Jarek, R. L.; Han, S. J. *Bull. Korean Chem. Soc.* **2002**, *23*, 267.
(7) Cho, Y. S.; Kim, M. S.; Choe, J. C. *Int. J. Mass Spectrom. Ion Processes* **1995**, *145*, 187.
(8) Choe, J. C.; Kim, M. S. *Int. J. Mass Spectrom. Ion Processes* **1991**, *107*, 103.
(9) Buschek, J. M.; Ridal, J. J.; Holmes, J. L. *Org. Mass Spectrom.* **1988**, *23*, 543.
(10) Baer, T.; Morrow, J. C.; Shao, J. D.; Olesik, S. *J. Am. Chem. Soc.* **1988**, *110*, 5633.
(11) McLafferty, F. W.; Winkler, J. *J. Am. Chem. Soc.* **1974**, *96*, 5182.
(12) McLafferty, F. W.; Bockhoff, F. M. *J. Am. Chem. Soc.* **1979**, *101*, 1783.
(13) Jackson, J. A. A.; Lias, S. G.; Ausloos, P. *J. Am. Chem. Soc.* **1977**, *99*, 7515.
(14) Traeger, J. C.; Kompe, B. M. *Int. J. Mass Spectrom. Ion Processes* **1990**, *101*, 111.
(15) Lifshitz, C.; Levin, I.; Kababia, S.; Dunbar, R. C. *J. Phys. Chem.* **1991**, *95*, 1667.
(16) Lin, C. Y.; Dunbar, R. C. *J. Phys. Chem.* **1994**, *98*, 1369.
(17) Lifshitz, C. *Acc. Chem. Res.* **1994**, *27*, 138.
(18) Lifshitz, C.; Gotkis, Y.; Ioffe, A.; Laskin, J.; Shaik, S. *Int. J. Mass Spectrom. Ion Processes* **1993**, *125*, 7.
(19) Moon, J. H.; Choe, J. C.; Kim, M. S. *J. Phys. Chem. A* **2000**, *104*, 458.
(20) Baer, T.; Hase, W. L. *Unimolecular Reaction Dynamics: Theory and Experiments*; Oxford: New York, 1996.
(21) Grotemeyer, J.; Grützmacher, H. F. *Current Topics in Mass Spectrometry and Chemical Kinetics*; Macoll, A. Ed.; Heyden: London, 1982; p 29.
(22) Grützmacher, H. F.; Harting, N. *Eur. J. Mass Spectrom.* **2003**, *9*, 327.
(23) Schulze, S.; Paul, A.; Weitzel, K.-M. *Int. J. Mass Spectrom.* **2006**, *252*, 189.
(24) Hwang, W. G.; Moon, J. H.; Choe, J. C.; Kim, M. S. *J. Phys. Chem. A* **1998**, *102*, 7512.
(25) Kim, Y. H.; Choe, J. C.; Kim, M. S. *J. Phys. Chem. A* **2001**, *105*, 5751.
(26) Choe, J. C. *J. Phys. Chem. A* **2006**, *110*, 7655.
(27) Choe, J. C. *Chem. Phys. Lett.* **2007**, *435*, 39.
(28) Frisch, M. J. ; Trucks, G. W.; Schlegel, H. B.; Scuseria, G. E.; Robb, M. A.; Cheeseman, J. R.; Montgomery Jr, J. A.; Vreven, T.; Kudin, K. N.; Burant, J. C.; Millam, J. M.; Iyengar, S. S.; Tomasi, J.; Barone, V.; Mennucci, B.; Cossi, M.; Scalmani, G.; Rega, N.; Petersson, G. A.; Nakatsuji, H.; Hada, M.; Ehara, M.; Toyota, K.; Fukuda, R.; Hasegawa, J.; Ishida, M.; Nakajima, T.; Honda, Y.; Kitao, O.; Nakai, H.; Klene, M.; Li, X.; Knox, J. E.; Hratchian, H. P.; Cross, J. B.; Bakken, V.; Adamo, C.; Jaramillo, J.; Gomperts, R.; Stratmann, R. E.; Yazyev, O.; Austin, A. J.; Cammi, R.; Pomelli, C.; Ochterski, J. W.; Ayala, P. Y.; Morokuma, K.; Voth, G. A.; Salvador, P.; Dannenberg, J. J.; Zakrzewski, V. G.; Dapprich, S.; Daniels, A. D.; Strain, M. C.; Farkas, O.; Malick, D. K.; Rabuck, A. D.; Raghavachari, K.; Foresman, J. B.; Ortiz, J. V.; Cui, Q.; Baboul, A. G.; Clifford, S.; Cioslowski, J.; Stefanov, B. B.; Liu, G.; Liashenko, A.; Piskorz, P.; Komaromi, I.; Martin, R. L.; Fox, D. J.; Keith, T.; Al-Laham, M. A.; Peng, C. Y.; Nanayakkara, A.; Challacombe, M.; Gill, P. M. W.; Johnson, B.; Chen, W.; Wong, M. W.; Gonzalez, C.; Pople, J. A. *Gaussian 03*, revision C.02; Gaussian, Inc.: Wallingford, CT, 2004.
(29) Scott, A. P.; Radom, L. *J. Phys. Chem. A* **1996**, *100*, 16502.
(30) Beyer, T.; Swinehart, D. R. *ACM Commun.* **1973**, *16*, 379.
(31) Choe, J. C. *J. Phys. Chem. A* **2006**, *110*, 4979.
(32) Kim, D. Y.; Choe, J. C.; Kim, M. S. *J. Phys. Chem. A* **1999**, *103*, 4602.
(33) Keister, J. W.; Baer, T.; Thissen, R.; Alcaraz, C.; Dutuit, O.; Audier, H.; Troude, V. *J. Phys. Chem. A* **1998**, *102*, 1090.
(34) Fridgen, T. D.; Troe, J.; Viggiano, A. A.; Midey, A. J.; Williams, S.; McMahon, T. B. *J. Phys. Chem. A* **2004**, *108*, 5600.
(35) Cone, C.; Dewar, M. J. S.; Landman, D. *J. Am. Chem. Soc.* **1975**, *99*, 372.
(36) Muntean, F.; Armentrout, P. B. *J. Phys. Chem. A* **2003**, *107*, 7413.

JP802641C